International Conferences on Recent Advances in Geotechnical Earthquake Engineering and Soil Dynamics

2010 - Fifth International Conference on Recent Advances in Geotechnical Earthquake Engineering and Soil Dynamics

26 May 2010, 4:45 pm - 6:45 pm

Lateral Response of Bridge Pile Groups in Liquefiable Soil with Surface Non-Liquefiable Layer Using Shaking Table Test

Tang Liang
Harbin Institute of Technology Harbin, China

Ling Xianzhang
Harbin Institute of Technology Harbin, China

Xu Pengju
Harbin Institute of Technology Harbin, China

Gao Xia
Harbin Institute of Technology Harbin, China

Recommended Citation

LATERAL RESPONSE OF BRIDGE PILE GROUPS IN LIQUEFIABLE SOIL WITH SURFACE NON-LIQUEFIABLE LAYER USING SHAKING TABLE TEST

Tang Liang
Harbin Institute of Technology
Harbin, Heilongjiang-China 150090

Ling Xianzhang, Xu Pengju, Gao Xia
Harbin Institute of Technology
Harbin, Heilongjiang-China 150090

ABSTRACT

This paper conducts a shaking table test study on seismic response of low-cap pile groups and bridge structure in liquefiable ground. The soil profile in the test consisted of the horizontal saturated sand layer overlaid the silty clay layer. The base was excited by three different El Centro earthquake events. The preliminary liquefaction characteristics of ground firstly were analyzed. The bending moment of the pile was mainly introduce in the note. There's no doubt that the shaking table test provided the necessary groundwork to study lateral response of bridge pile groups in liquefiable soil with surface non-liquefiable layer.

INTRODUCTION

One of the main causes of earthquake-induced damage to the piles is the occurrence of soil liquefaction, and the significance of liquefaction-related damage to the piles has been clearly demonstrated in many earthquakes such as the 1995 Hyogo-ken Nambu Earthquake of Japan, the 1976 Tangshan Earthquake of China and so on. Although soil liquefaction might reduce the inertial force of the superstructure, the damage to the superstructure was often ascribed to the damage of the piles (Fujii et al., 1998; Finn et al., 2002). So that it is important to consider seismic soil-pile-structure interaction in seismic design of the piles particularly in liquefiable ground. However, since less attention has been paid to the behavior of this type of pile groups in the past, there is currently only limited information available regarding seismic response of low-cap pile groups and bridge structures in liquefiable ground (Abdoun et al., 2002; Boulanger et al., 1999). Nowadays, this type of piles is widely adopted in bridge engineering, especially bridges built in special ground consisting of liquefiable soils. There are few physical modeling data available for understanding the mechanisms of soil-low-cap pile groups-bridge structure interaction in liquefied soil, nor are there procedures available for the design of this type of pile groups (Li et al., 2004; Ling et al., 2004).
A shaking table test was conducted in 2006; it helped to gain insight into the mechanisms of seismic soil-pile-structure interaction under the condition of low-cap pile groups and obtain dynamic behavior of pile groups and bridge structure in liquefiable ground. Meanwhile, one of the key tasks of this test was to generate reliable data, which could be used to improve analysis techniques and design guidelines for low-cap pile groups. In this paper, the liquefaction characteristics of ground and the bending moment on the pile in the test are presented and analyzed.

SHAKING TABLE TEST

Shaking table test was performed at the State Key Laboratory for Disaster Reduction in Civil Engineering, Tongji University, Shanghai, China, using MTS shaking table facility. The dimension of the table was 4 m×4 m, and the maximum payload was 25, 000 kg. The large-scale laminar shear box was 2 m high, 1.5 m wide and 2 m long (shaking direction) on the shaking table. The shear box was designed to be sufficiently light compared with the model. Therefore, the shear box produced nearly one-dimensional wave propagation fields, i.e. free-field conditions. The soil profiles used in the test consisted of two horizontal soil layers.
The test sand, with a non-uniformity coefficient of 3.0, mean particle diameter of 0.32 mm, specific gravity of 2.72, maximum void ratio of 0.96, minimum void ratio of 0.57 and maximum diameter of 2 mm, was obtained in Shanghai, China. The laminar shear box was partially filled with water in advance, and after that, the sand without being washed was directly placed into the laminar shear box, using a free fall method for the saturated sand layer (Ling et al., 2005). The

sand was lifted to a certain height and dropped into the box through a cone. The dropping height related to the relative density was determined according to the required relative density. Efforts were made not to densify the sand layer and prepare the homogeneous sand layer as much as possible. The height of the lower sand layer with average void ratio of 0.8, relative density of 60% and permeability coefficient of about 0.0035 cm/s prepared was 1.6 m. This method for the saturated sand was successfully used in the previous model studies (Ling et al., 2004). The upper layer of 0.3 m thickness was normally consolidated reconstituted silty clay for the "model clay". The model clay had liquid and plastic limits of LL 45 and PL 28, and a plasticity index of PI 17. In order to ensure the sand layer completely submerged, the water table was approximately at the soil interface between the upper clay layer and lower saturated sand layer.
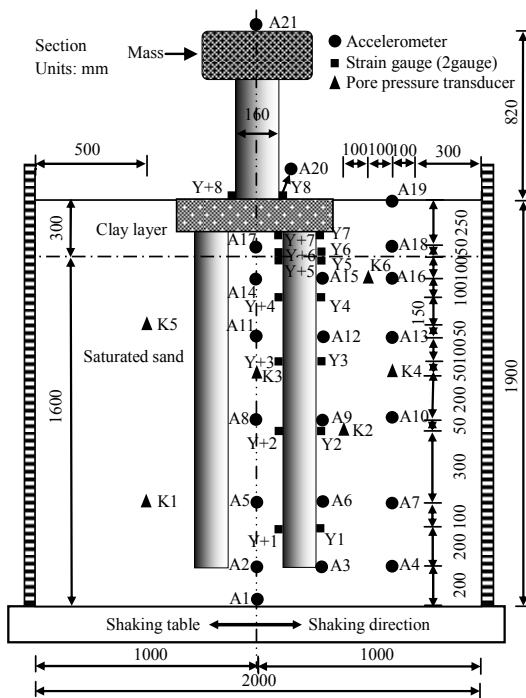

Fig. 1 Schematic figure of whole test system

A low-cap four-pile group with single pier was used in the test. The reinforced concrete piles, cap and column pier were modeled with fine-aggregate concrete and galvanized fine iron wires. All the bars embedded in the model structure were replaced by galvanized iron wire with different diameters and had the same bar mark "Φ". The vertical reinforcements, which consisted of 9 Φ2 bars and evenly distributed around a circle with a diameter of 70 mm, were embedded in each pile with a diameter of 80 mm. The confinement to the vertical steel was provided by Φ1 bar spirals with a pitch of 20 mm, especially with a pitch of 10 mm within the range of 600 mm of the piles near the cap. A 5 mm concrete cover of the piles was maintained to protect the reinforcement bars. The vertical reinforcement of the pier with 160 mm diameter consisted of

32 Φ2 bars evenly distributed around a circle with a diameter of 150 mm, and the confinement to the vertical steel was provided by Φ1 bar spirals with a pitch of 20 mm especially with a pitch of 10 mm within the range of 150 mm of the pier bottom. A 5 mm concrete cover of the pier was still maintained. Besides, pile groups were lined up 2 by 2 with a spacing of 3.75 times diameter of the pile. Based on the concrete material specimen tests, the fine-aggregate concrete had an average 28-day compressive strength of 8.5 MPa. Considering the fact that the simply supported beam bridges were usually used in bridge engineering, the superstructure in the test was substituted by the individual mass of 360 kg on the top of the pier to characterize the inertial effect of bridge structure.

Detailed constructions of the shaking table test including the layout of the measure transducers, the geometry and the pile groups system are shown in Fig.1. The model structure had been installed into the laminar shear box before the laminar box was filled with the test sand. The pile tip was located in the sand at the depth of 1700 mm. Measurement system, which basically consisted of 8 pair of strain gauges attached on the pile and the pier bottom, 21 accelerometers in the soil and on the pile and 6 pore pressure transducers in the sand layer, was described in Fig.1. A pair of strain gauges was fixed on the piles at the same depth. The accelerometers in the soil layer were placed in the perspex boxes, which could ensure to follow the movement of the soil layer simultaneously during shaking.

In order to avoid the disadvantageous effect for the test, the container base was only excited by three El Centro earthquake events, summarized in Table 1. The suite of shaking events began with the very low-level shaking events to characterize the low-strain response of soil and soil-structure system and then successively progressed through very strong motions to bring the piles into the nonlinear stage and soil liquefaction. In order to investigate the effect of the frequency component of the input shaking acceleration on soil liquefaction, event B was scaled by the time scaling factor of $1/\sqrt{10}$ relative to event C. The dominant frequency of the input shaking acceleration between event B and event C was apparently different. Events C and D had the peak amplitude of 0.15g and 0.5g occurring at the same time, respectively. The interval between two shaking events was long enough to dissipate the excess pore pressure generated in last event.

Table 1. Suite of Shaking Events

Event	Motion	A_{max} base input (g)
A	White noise	0.002
B	Scaled El Centro earthquake (NS)	0.15
C	El Centro earthquake (NS)	0.15
D	El Centro earthquake (NS)	0.5

TEST RESULTS

Liquefaction Characteristics of Ground

Time histories of excess pore pressure ratios are presented in Fig.2 for various depths throughout the sand profile from three earthquake events. Compared with that in event C, excess pore pressure ratio were relatively smaller in event B, which indicated that the duration of earthquake seemed to have noticeable effect on the pore pressure generation. The maximal excess pore pressure ratio gradually decreased but obtained the value between 0.2 and 0.3 from bottom to top in the vertical direction in event B, which well agreed with the phenomenon that the waterspouts didn't appear on the ground surface. Excess pore pressure ratio gradually decreased but obtained the value at about 0.4 to 0.5 bottom-up in the vertical direction in event C. The sand sample in the laboratory testing might come forth the light soil liquefaction when excess pore pressure ratio ranged between 0.3 and 0.7. According to the research findings and the observed phenomena in the test, that also showed that slight soil liquefaction occurred in the sand

in event C. The excess pore pressure ratio rapidly increased and exceeded 1.0 from bottom to top in the vertical direction in event D. After reaching its peak, excess pore pressure ratios maintained the level for the 30 to 50 seconds time and didn't immediately reduce, which illustrate the reason for keeping for a long time of liquefaction. The time when excess pore pressure ratio quickly increased was near the peak time of the input shaking acceleration, but the peak excess pore pressure ratio exhibited obvious time lag in different earthquake events, which was more distinct in event D. The time when the maximum excess pore pressure ratios of the sand layer appeared were almost consistent in the same earthquake event. Therefore, the strongest liquefaction lagged behind the input peak shaking acceleration. Note that excess pore pressure ratios was also highly determined by the magnitude of the input shaking acceleration. Meanwhile we also obtained that the excess pore pressure accumulated slowly during small-amplitude shaking at the early stage of events B, C and D, but the obvious accumulation of excess pore pressure was observed at the strongest shaking stage in event B, C and D.
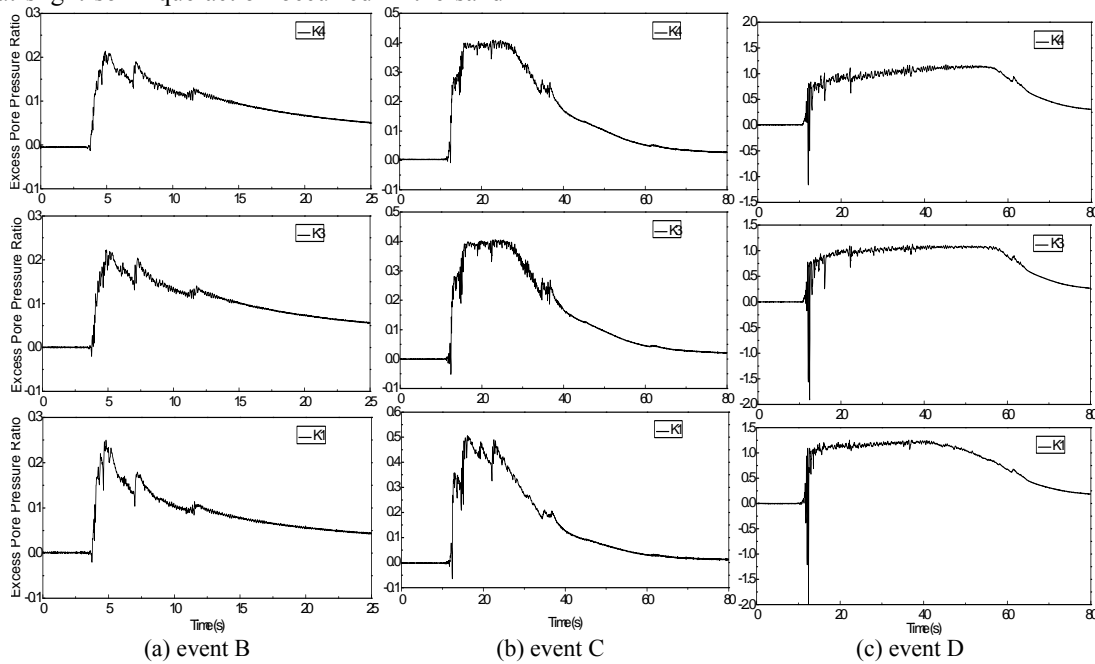

(a) event B   (b) event C   (c) event D

Fig. 2. Time histories of excess pore pressure ratios from three earthquake events

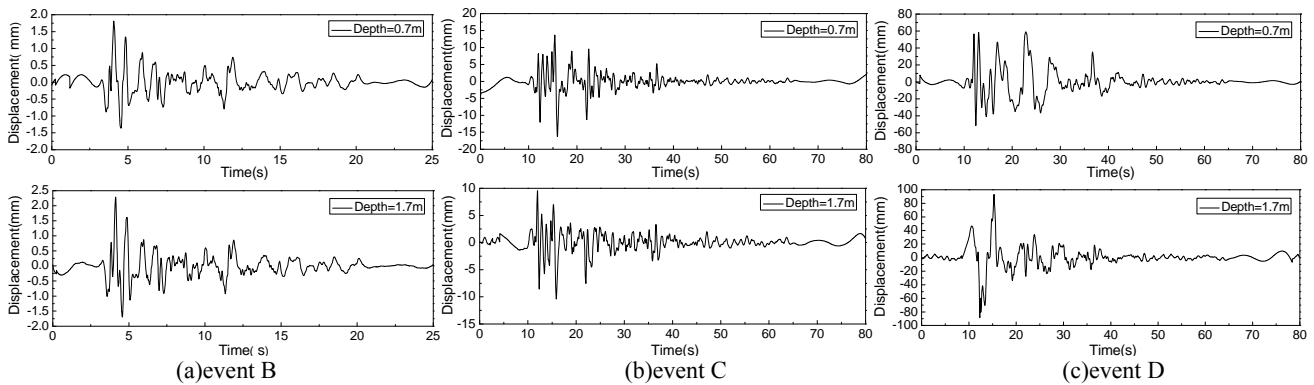(a)event B   (b)event C   (c)event D

Fig. 2. Displacement time histories of sand under three earthquake events

Displacement time histories of the sand obtained by double-integrating the accelerometers of the vertical array in the soil profile far away the piles are depicted in Fig.3 under three earthquake events. In event B, the peak time of the sand displacement and the input shaking acceleration was almost simultaneous. In events C and D, the time when the peak displacement of sand reached the peak lagged behind the input peak shaking acceleration. Note that the displacement of the fully liquefied sand in the upper sand kept the higher value for a long time in event D, which might be caused by the intense come-and-go shear flow action of liquefied sand.
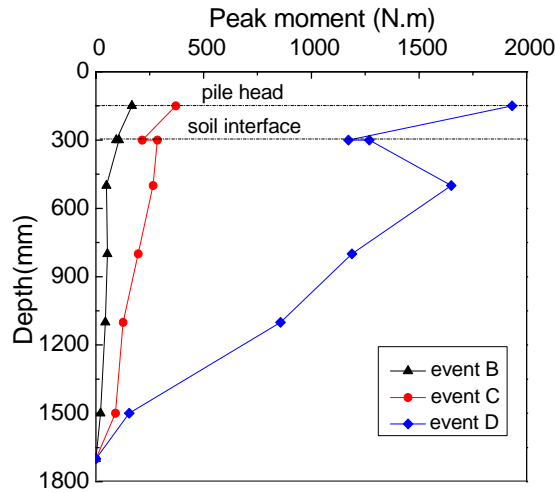

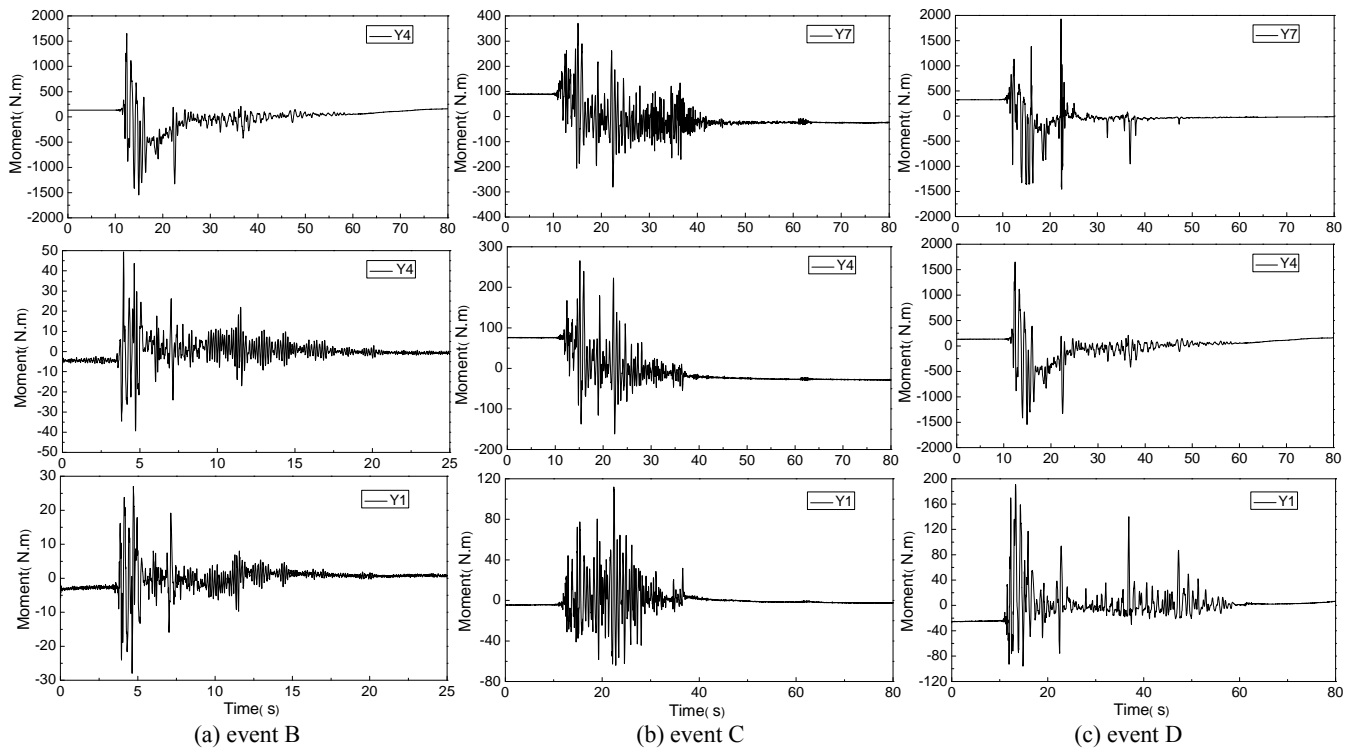Fig. 4. Peak moment on the pile along the depth in events B, C and

(a) event B   (b) event C   (c) event D

Fig. 5. Moment time histories of the pile in events B, C and D

Bending Moment of Pile

The strain measurements along the length of the pile had to be converted into the curvature and moment data. From beam mechanics, it's known that strain, ε, was proportional to the curvature, k, and varied linearly with distance, h, from the neutral axis. A rearrangement of the strain-curvature relationship provided the following equation for the curvature:

$$k = \frac{\varepsilon}{h} \qquad (1)$$

It should be recognized that the curvature was based solely on geometry and not material properties; therefore, equation 1 was valid for linear as well as non-linear elastic materials. When both sides of a symmetric pile were instrumented, the above equation became:

$$k = \frac{\varepsilon_t - \varepsilon_c}{2h} \qquad (2)$$

where the subscripts t and c distinguish the strains measured on the tension and compression sides of the pile (with opposite signs), respectively. In the case of a round cross-section with gauges mounted to the exterior of the pile, the term $2h$ was equal to the diameter of the pile. After determining the curvature, the structural and material properties of the pile could then be used to determine the moment. The peak moment along the pile is presented in Fig.4 and the time histories of the moment on the pile are depicted in Fig.5 and in events B, C and D. It's clearly indicated that the moment on the pile in the sand gradually increased from bottom to top in events B and C and the moment on the pile was larger in event C than in event B. The time of the peak moment consisted with the peak input shaking acceleration time of about 12 seconds in event B. The time of the maximum moment well agreed with that of the peak sand displacement in event C, which was the same trend in event D. The moment of the pile first gradually increased and then decreased bottom-up in the sand in event D. In three earthquake events, though the abrupt change of the moment was found near the soil interface, the peak moment existed in the pile heads. These facts indicated that the restriction from the upper clay layer and the cap on the pile heads were quite effective and the minimum moment occurred in the pile bottom because the pile tip wasn't fixed. Compared with the peak time of the sand displacement, the input shaking acceleration and the moment of the pile, it's acquired that the soil deformation had a more and more obvious effect on the moment of the pile with the development of soil liquefaction. It's concluded that the amplitude of the input shaking acceleration and the inertial effect of the superstructure might notably control the moment response of the pile when the excess pore pressure ratio was less than 0.3 in event B. The soil deformation began to remarkably influence the moment on the pile when the excess pore pressure distinctly increased and the soil gradually displayed the liquefied characteristic in events C and D, especially in event D. Therefore, the special attention of the contribution from the liquefied sand to the piles and the peak moment on the pile heads of low-cap pile groups should be paid to seismic design of bridge piles in liquefiable ground.

REFERENCES

Abdoun, T. and Dobry, R. [2002]. "Evaluation of Pile Foundation Response to Lateral Spreading," *Soil Dynamics and Earthquake Engineering,* No. 22, pp. 1051-1058.

Bhattacharya, S. [2003]. "Pile Instability during Earthquake Liquefaction," *ph.D. Dissertation*, University of Cambridge, Cambridge.

Boulanger, R.W., Curras, C.J., Kutter, B.L., et al. [1999]. "Seismic Soil-Pile-Structure Interaction Experiments and Analyses," *Journal of Geotechnical and Geoenvironmental Engineering*, No. 9, pp. 750-759.

Fujii, S., Cubrinovski, M., Tokimatsu, K., et al. [1998]. "Analyses of Damaged and Undamaged Pile Foundations in Liquefied Soils During the 1995 Kobe Earthquake," *Proc. 3rd Conf. Geotechnical Earthquake Engineering and Soil Dynamics*, ASCE, Seattle, pp. 1187-1198.

Finn, W.D.L. and Fujita, N. [2002]. "The Piles in Liquefiable Grounds: Seismic Analysis and Design Issues," *Soil Dynamics and Earthquake Engineering*, No. 22, pp. 731-742.

Kagawa, T., Minowa, C., Mizuno, H., et al. [1994]. "Shaking-Table Tests on Piles in Liquefying Sand," *Proc. 5th U.S. Natl. Conf. Earthquake Eng.*, Chicago, No. 4, pp. 107-116.

Li, Y.R. and Yuan, X.M. [2004]. "State-of-art of Study on Influences of Liquefaction-induced Soil Spreading over Pile Foundation Response," *World Earthquake Engineering*, No. 2, pp.17-22. (in Chinese)

Ling, X.Z., Wang, C. and Wang, C. [2004]. "Scale Modeling Method of Shaking Table Test of Dynamic Interaction of Pile-Soil-Bridge Structure in Ground of Soil Liquefaction," *Chinese Journal of Rock Mechanics and Engineering*, No. 3, pp. 450-456. (in Chinese)

Ling, X.Z., Wang, L.X., Wang, D.S., et al. [2005]. "Study on Large-scale Shaking Table Proportional Model Test of the Dynamic Property of Foundation in Unfree Ground of Liquefaction," *China Journal of Highway and Transport*, No. 2, pp. 34-39. (in Chinese)